Mechanism of Alamethicin Insertion into Lipid Bilayers

Ke He, Steve J. Ludtke, William T. Heller, and Huey W. Huang
Physics Department, Rice University, Houston, Texas 77005-1892 USA

ABSTRACT Alamethicin adsorbs on the membrane surface at low peptide concentrations. However, above a critical peptide-to-lipid ratio (P/L), a fraction of the peptide molecules insert in the membrane. This critical ratio is lipid dependent. For diphytanoyl phosphatidylcholine it is about 1/40. At even higher concentrations P/L $\geq$ 1/15, all of the alamethicin inserts into the membrane and forms well-defined pores as detected by neutron in-plane scattering. A previous x-ray diffraction measurement showed that alamethicin adsorbed on the surface has the effect of thinning the bilayer in proportion to the peptide concentration. A theoretical study showed that the energy cost of membrane thinning can indeed lead to peptide insertion. This paper extends the previous studies to the high-concentration region P/L > 1/40. X-ray diffraction shows that the bilayer thickness increases with the peptide concentration for P/L > 1/23 as the insertion approaches 100%. The thickness change with the percentage of insertion is consistent with the assumption that the hydrocarbon region of the bilayer matches the hydrophobic region of the inserted peptide. The elastic energy of a lipid bilayer including both adsorption and insertion of peptide is discussed. The Gibbs free energy is calculated as a function of P/L and the percentage of insertion ϕ in a simplified one-dimensional model. The model exhibits an insertion phase transition in qualitative agreement with the data. We conclude that the membrane deformation energy is the major driving force for the alamethicin insertion transition.

INTRODUCTION

Alamethicin is a 20-amino acid, antibiotic peptide produced by the fungus *Trichoderma viride* (Meyer and Reusser, 1967; Pandey et al., 1977). Recent experiments have clarified the mode of alamethicin's cytolytic action. One important feature of its antibacterial activity is that there are minimum alamethicin concentrations that are required to inhibit growth (or cause cellulolysis) of various organisms. These concentrations are at least two orders of magnitude greater than the concentration required to induce voltage-dependent conductivity in lipid bilayers (Jen et al., 1987). Indeed, the channeling activities of alamethicin observed in the conductivity measurements are transient fluctuation phenomena occurring when the great majority of the peptide is adsorbed on the bilayer surface (Latorre and Alvarez, 1981; Mak and Webb, 1995; and references cited therein). However, there is a lipid-dependent critical concentration above which a finite fraction of alamethicin is inserted into the bilayer. And above an even higher concentration, the great majority of the alamethicin molecules are all inserted (Huang and Wu, 1991). Neutron in-plane scattering of the inserted phase showed that alamethicin forms large, well-defined pores in membranes (He et al., 1995, 1996). This result supports our hypothesis that the insertion transition is the molecular mechanism of alamethicin's cytolytic activity (Ludtke et al., 1994). In previous papers we discussed what causes the onset of the insertion transition. X-ray diffraction studies (Wu et al., 1995) showed that adsorption of alamethicin on the membrane surface causes membrane thinning. The energy cost of membrane thinning raises the free energy of the surface state to exceed that of the inserted state at high concentrations (Huang, 1995). In this paper we discuss what causes all of the peptide to become inserted. We will show the result of x-ray lamellar diffraction in the coexistence phase and the insertion phase. We will also discuss the energetics of the insertion transition based on observed changes in the membrane thickness.

When alamethicin is associated with a lipid bilayer, its circular dichroism (CD) spectrum is dominated by a helical signal (Vogel, 1987; Olah and Huang, 1988). Furthermore, this spectrum has an orientational dependence characteristic of a pure helix (Wu et al., 1990). Thus it is easy to use CD to detect the orientation of alamethicin molecules in an oriented sample. Alamethicin associated with diphytanoyl phosphatidylcholine (DPhPC) bilayers at various peptide lipid molar ratios (P/L) was examined by this method (Huang and Wu, 1991; Wu et al., 1995) for its helical orientation. Fig. 1 shows the helical orientation at different P/L (Huang et al., 1995). The orientation also depends on the degree of hydration. Here we will discuss only the concentration dependence at full hydration, for this is most relevant to the physiological condition. The hydration dependence will be discussed in future publications.

In the previous x-ray study we found that for peptide concentrations P/L = 1/47 and below, the bilayer thickness decreases linearly with the peptide concentration. This result was interpreted as evidence that the peptide is adsorbed within the headgroup region of the bilayer. The adsorption expands the bilayer laterally and hence reduces its thickness. From the thickness reduction one can calculate the areal expansion per peptide, and the value indeed corresponds to the area of an adsorbed alamethicin (Wu et al., 1995). The energetics of membrane thinning was then discussed in terms of an elasticity theory of lipid bilayers, with

Received for publication 20 May 1996 and in final form 2 August 1996.
Address reprint requests to Dr. Huey W. Huang, Department of Physics, Rice University, Houston, TX 77005-1892. Tel.: 713-527-4899; Fax: 713-527-9033; E-mail: huang@ion.rice.edu.

0006-3495/96/11/2669/11 $2.00

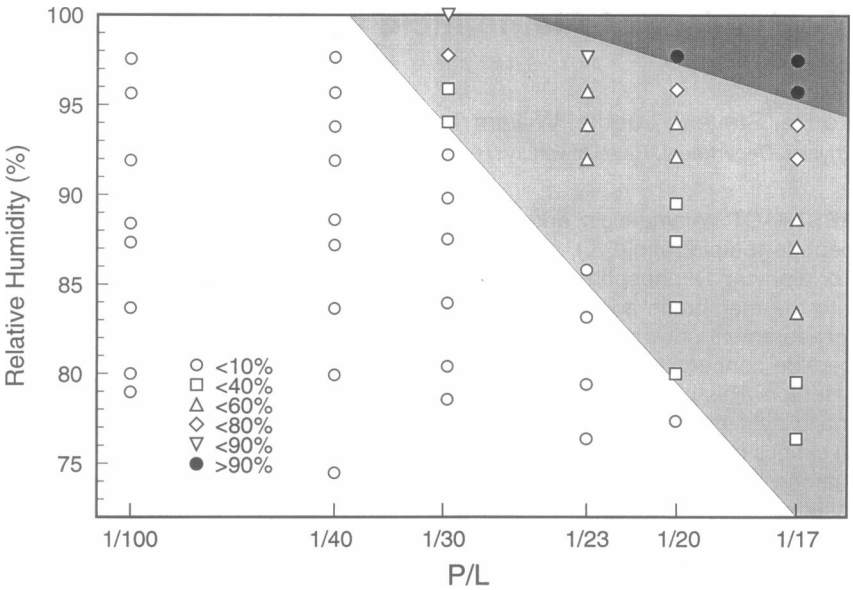

FIGURE 1 Phase diagram of alamethicin orientation in DPhPC bilayers. The orientation was determined by OCD. The helical orientation parallel to the plane of the bilayers represents the surface state. The helical orientation normal to the plane of the bilayers represents the inserted state. Partially inserted states are determined by spectral decomposition. The symbols represent percentages of insertion.

two major conclusions (Huang, 1995): 1) The adsorbed monomers repel each other if the interpeptide distance is less than an interaction distance (about 40 Å). Therefore the peptide is dispersed on the bilayer surface as monomers. At low concentrations the energy of adsorption (per peptide) is independent of the concentration. 2) However, if the concentrations are such that the average interpeptide distance is less than the interaction distance, the total free energy of membrane deformation increases with the square of the peptide concentration. This explains the instability of the surface state at high peptide concentrations and hence the onset of insertion transition, but it does not explain why all of the peptides become inserted at even higher concentrations.

INSERTION TRANSITION IS NOT A MICELLIZATION EFFECT

Neutron in-plane scattering shows that alamethicin in the inserted state aggregates to form discrete pores, each consisting of about 11 monomers (He et al., 1995, 1996). Because aggregation and phase transition are both cooperative phenomena, one might ask if the insertion transition is simply a manifestation of the cooperativity embodied in the aggregation process. We show here that this is not the case. Aggregation is the same as micellization, the result of a kinetic equilibrium between the monomeric state and oligomeric states (e.g., Blankschtein et al., 1986). Although there is a so-called critical micellization concentration (CMC), it is not a phase transition. This is best illustrated with a two-state model (Blankschtein et al., 1986). Let C_1 be the concentration of the surface monomers, C_n the concentration of the pores, each made of n monomers, and C the total peptide concentration. Then the chemical equilibrium between the monomers and the pores implies

$$C_n = C_1^n e^{-\beta(\mu_n - n\mu_1)}, \tag{1}$$

where μ_i and μ_n are the chemical potential of the monomers and the pores, respectively, and $\beta = (k_B T)^{-1}$. Defining $C_c = \exp\{\beta[(\mu_n - n\mu_1)/(n-1)]\}$, we can express $C = C_1 + nC_n$ as

$$\frac{C}{C_c} = \frac{C_1}{C_c} + n\frac{C_n}{C_c} = \frac{C_1}{C_c} + n\left(\frac{C_1}{C_c}\right)^n. \tag{2}$$

As determined by neutron in-plane scattering, the size of alamethicin pores in DPhPC bilayers is $n = 11$. Clearly, for $C \ll C_c$ we find $C \approx C_1$. All of the added peptide appears in the monomeric state. But for $C \gg C_c$ the pore term dominates. In fact, C_1 needs to exceed C_c by only a very small amount in order that almost all of C-C_c be accommodated entirely in the pore state. Thus as soon as C exceeds C_c, practically all of the added peptide will be inserted in the pore state with very little change in the monomer concentration. C_c is called the CMC.

However, this picture does not describe our phase diagram (Fig. 1). If the peptide insertion transition were a micellization phenomenon, the CMC would be about P/L = 1/40. Then at P/L = 1/15 one would expect about 5/8 of the peptide to be inserted and 3/8 to remain on the surface. Instead, experiment showed that at P/L = 1/15 all of the peptide is inserted. Thus the insertion transition is a phase transition rather than a micellization effect.

EXPERIMENT

Oriented circular dichroism

The materials used in this experiment are the same as in the previous experiment (Wu et al., 1995). 1,2-Diphytanoyl-3-phosphatidylcholine (DPhPC) in $CHCL_3$ was purchased from Avanti Polar Lipids (Alabaster, AL). Alamethicin was purchased from Sigma Chemical Co. (St. Louis, MO). Ori-

ented multilayers of peptide-lipid mixtures were prepared on the surface of a quartz slide. The technique for preparing an oriented sample on one substrate has been described previously (Ludtke et al., 1994). The open-faced sample allows a rapid change of sample hydration. Oriented circular dichroism (OCD) was measured with light incident normal to the substrate in a Jasco J-500A spectropolarimeter (Wu et al., 1990). In the coexistence (i.e., partially inserted) region, the spectrum was fit by a linear superposition of the inserted spectrum and the surface spectrum (Wu et al., 1990). The fit coefficients were used to calculate the percentage of insertion.

X-ray diffraction

Materials and methods were unchanged from the previous experiment (Wu et al., 1995), with the exception of an improved humidity control. Oriented smectic liquid crystals of DPhPC bilayers containing alamethicin at P/L = 1/30, 1/23, 1/20, and 1/15 were prepared between a quartz slide and a SiO_2 coated Be plate. Diffraction patterns were measured by ω-2θ scan from the Be side. The x-ray sample was housed in a temperature-humidity chamber equipped with a water source. The temperatures of the sample and the water source were each controlled by a Peltier thermoelectric module (Melcor, Trenton, NJ), which functioned as a heater/cooler. High (low) humidities were achieved by raising (lowering) the water temperature slightly above (below) that of the sample ($-5°C < \Delta T < 2°C$). The temperatures were electronically monitored and feedback controlled. All measurements were performed at the sample temperature, 25°C. Each sample was scanned through a wet-dry-wet cycle.

Fig. 2 shows the diffraction patterns of DPhPC bilayers containing high concentrations of alamethicin. Three ranges of repeat distance (D) are shown: the wet region ($D > 49$ Å), the middle region (49 Å $> D >$ 46 Å), and the dry region (46 Å $> D$). We follow the procedure of data reduction described in Wu et al. (1995). A representative phasing diagram (scattering amplitude versus momentum transfer) is shown in Fig. 3. As noted in the low concentration experiment (Wu et al., 1995), the lipid apparently underwent a lyotropic phase transition upon dehydration. The phasing diagram shows a discontinuous change through the middle region (*arrows* in Fig. 3). In the case of P/L = 1/20 and 1/15, the diffraction intensity was greatly reduced in the middle region, as if the samples became disordered. However, above and below this region the intensities were equally strong. The loss and the recovery of diffraction power occurred during dehydration and recurred during hydration. After the phase determination, the relative scattering amplitudes were Fourier-transformed to obtain the scattering density profile. We define the peak-to-peak distance in the profile as the bilayer thickness t (Wu et al., 1995; Ludtke et al., 1995).

A very serious concern of membrane diffraction experiments is that sample disorders might have influenced the diffraction intensity. Disorders are either of static or dynamic origins. Static disorder is the result of defects in the

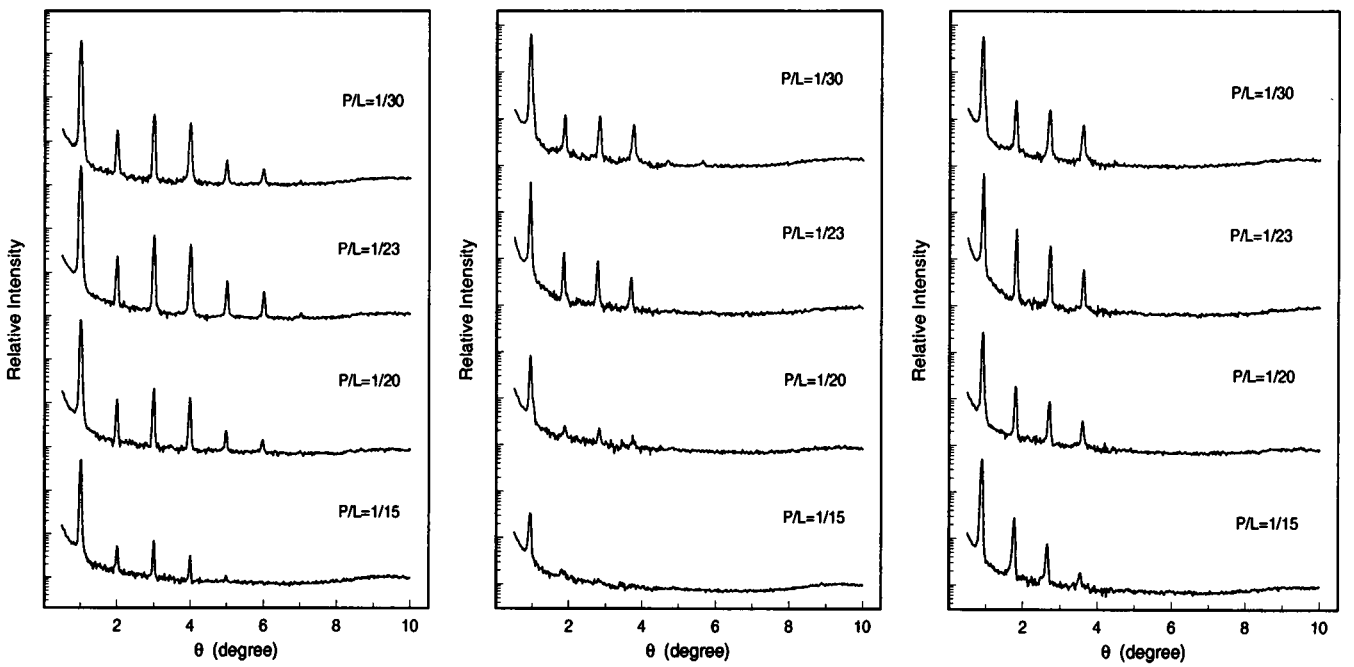

FIGURE 2 Diffraction patterns of DPhPC bilayers containing high concentrations of alamethicin. At P/L = 1/30, 1/23, 1/20, and 1/15, alamethicin is either partially inserted or completely inserted. A typical pattern for each P/L is shown in three regions of repeat spacing D. $D > 49$ Å (*right*) is the wet region just below the full hydration. In this region, the samples exhibited oily streak defects under polarized microscopy, indicating the L_α phase (Asher and Pershan, 1979; Huang and Olah, 1987). The lipids underwent a lyotropic phase transition upon dehydration in the middle region, 49 Å $> D >$ 46 Å (*middle*). The lipids were in a gel phase in the dry region, $D <$ 46 Å (*left*).

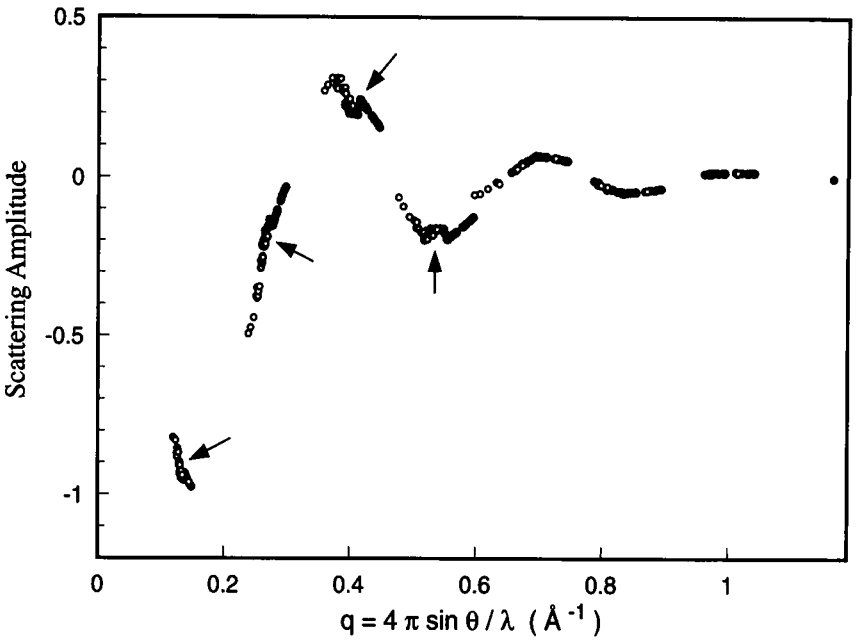

FIGURE 3 A representative phasing diagram, scattering amplitude versus momentum transfer q. Circles are the wet region. The black dots are the middle and dry regions. If the bilayer structure is unchanged or changing slightly and continuously during dehydration, the scattering amplitudes would fall into a smooth curve. A discontinuous kink (*arrows*) indicates a phase transition.

membrane alignment. They can be minimized by standard procedures (Asher and Pershan, 1979; Huang and Olah, 1987). These procedures were applied to our samples before the x-ray experiment. Dynamic disorder is the result of thermal fluctuations. Its effect on diffraction has been theoretically calculated and experimentally demonstrated (Caillé, 1972; Nallet et al., 1993; Zhang et al., 1994; Lei et al., 1995). Most importantly, thermal fluctuations are greatly reduced if the multilayers are dehydrated to less than ~98% relative humidities (Wu et al., 1995; Nagle et al., 1996). These are our experimental conditions. Once fluctuations are small, another property of lipid bilayers makes the peak-to-peak distance relatively insensitive to the effect of fluctuation. We show this property in Appendix I (i.e., because the scattering density profile is approximately symmetrical near the peak, fluctuations have a diminished effect on t). This was demonstrated previously with real data by Nagle et al. (1996). Thus we had reasons to expect our measurement to be relatively free of the artifact of sample disorders.

Fig. 4 shows the peak-to-peak distance t versus the lamellar repeat distance D. We note that the data points in the dry region, $D < 47$ Å, fall into a universal line. In fact, the data from the low concentration experiment, for P/L = 1/47 and for P/L = 0 (Wu et al., 1995), also overlap this universal line in the dry region. This indicates that in the dry

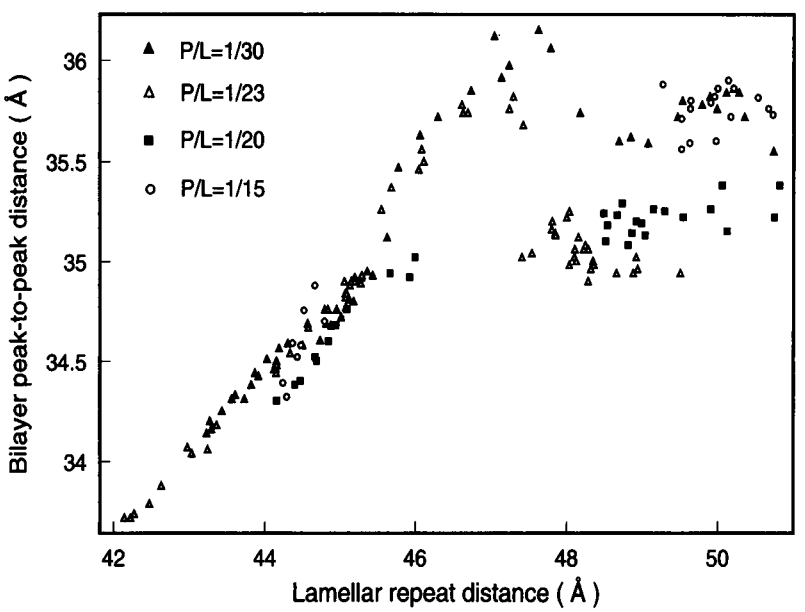

FIGURE 4 Peak-to-peak distance t versus lamellar repeat distance D for four different peptide concentrations.

region the lipid is in a well-defined gel phase, independent of the peptide concentration. (The peptide is probably not incorporated into the bilayer, not even in the headgroup region. OCD indicated that in this region the peptide is oriented parallel to the plane of the bilayer.) For the problem under consideration, the most important conclusion from the data of the dry region is that our results are free of the possible effect of sample disorders. Otherwise the effect of defects should vary from sample to sample and the data from different peptide concentrations would not overlap with each other in the dry region. Therefore the decrease in the number of discernible Bragg peaks in the wet region, from 6–7 at low peptide concentrations (P/L $\leq$ 1/47) to 4 at high peptide concentrations (P/L $\geq$ 1/30), must be the result of changes in the bilayer structure (the form factor) rather than due to higher degrees of disorder in high peptide concentrations.

In the wet region the peak-to-peak distance is independent of D spacing, and each peptide concentration produces a distinct average bilayer thickness. This was also true in another peptide-lipid system (magainin in palmitoyl-oleoyl-phosphatidylcholine/serine mixture; Ludtke et al. 1995), that is, the bilayer thickness approaches a constant value as the water content approaches full hydration. Thus we may use the bilayer thickness measured at relative humidities slightly less than 100% to infer its value at full hydration. This finding is supported by Nagle et al. (1996), who showed that the bilayer structure of dipalmitoyl-phosphatidylcholine is unchanged from full hydration to 98% relative humidity. We plot the average bilayer thickness in the wet region versus P/L, including the low concentration data from the previous experiment, in Fig. 5. Fig. 6 shows the corresponding percentage of insertion versus P/L, also near full hydration. We see that as long as alamethicin is adsorbed on the surface, the bilayer thickness decreases in proportion to the peptide concentration. However, once the insertion occurs, the pattern of thickness change is different. At least it is clear that as the percentage of insertion approaches 100%, the membrane thickness increases with the peptide concentration. We assume that this is because the hydrocarbon region of the bilayer matches the hydrophobic region of the inserted peptide. Therefore the membrane thickness is fixed by the inserted peptide at the contact point. Thus alamethicin adsorption on the surface causes membrane thinning, but alamethicin insertion causes the membrane thickness to approach a fixed value. In the next section we will show that these two mechanisms can cause the peptide insertion transition.

THEORY

To discuss the energetics of membrane thinning, we use a continuum theory that at the molecular scale can be regarded as a mean field theory (e.g., Huang, 1963). A mean field theory gives a qualitative description of averaged molecular properties. Our goal here is to understand if the peptide insertion transition is driven by the membrane deformation energy. We start with a bilayer deformation energy, per unit area of the unperturbed system, given by (Huang, 1995)

$$f = aB\left[\frac{D(x, y)}{2a}\right]^2 + \frac{K_c}{8}[\Delta D(x, y)]^2 + \frac{K_c}{2}[\Delta M(x, y) - C_o(x, y)]^2. \quad (3)$$

The unperturbed bilayer is assumed to lie on the xy plane. $D(x,y)$ is the deviation of the bilayer thickness from the equilibrium thickness $2a$ at the coordinate (x, y). $M(x, y)$ is the displacement of the midplane of the bilayer from its equilibrium position. Δ is the Laplacian $\partial^2/\partial x^2 + \partial^2/\partial y^2$. B

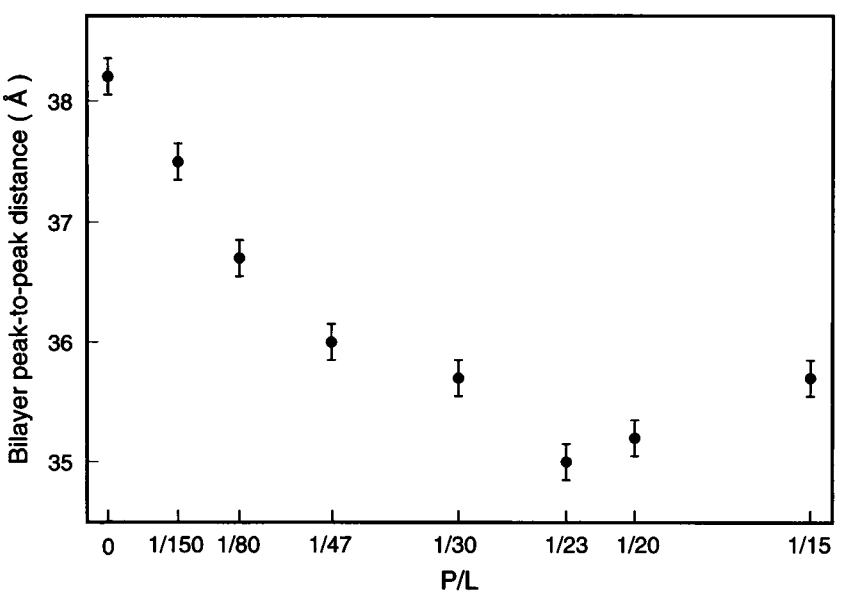

FIGURE 5 Bilayer thickness in the wet region versus P/L. The points represent the average values and the error bars represent the standard deviations of the data shown in Fig. 4. The low concentration data (P/L $\leq$ 1/47) are from Wu et al. (1995).

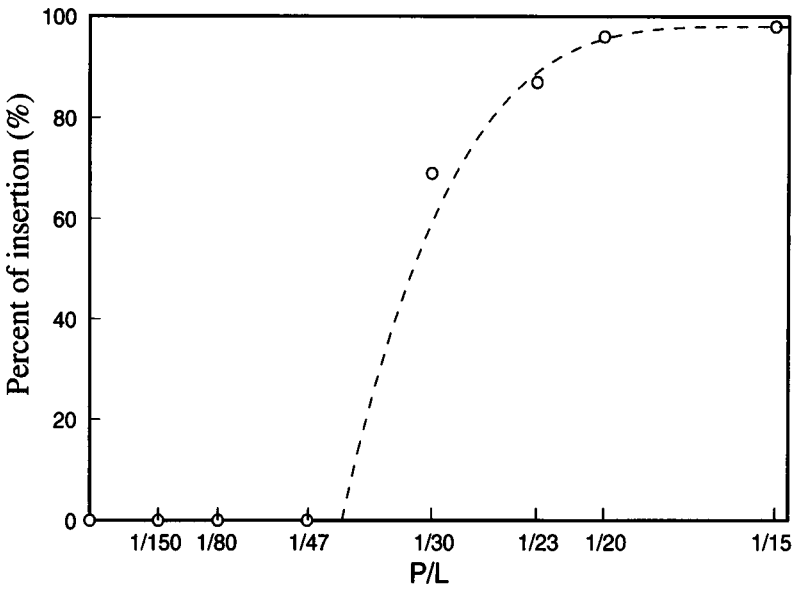

FIGURE 6 Percentage of insertion versus P/L near full hydration from Fig. 1. The dashed line is a guide for the eye.

is the compressibility modulus of the bilayer. K_c is Helfrich's bending rigidity for a bilayer (Helfrich, 1973). $C_o(x, y)$ is the local spontaneous curvature induced by peptide adsorption. Only the change of the bilayer thickness (the D mode) will concern us here. The free energy of thickness deformation consists of only the first two terms, the compressibility term and the splay term. Minimization of the free energy gives the differential equation

$$\frac{1}{\lambda^4} D(x, y) + \Delta^2 D(x, y) = 0, \tag{4}$$

where $\lambda = (aK_c/2B)^{1/4}$ is the length scale of thickness deformation. With appropriate boundary conditions, the solution of Eq. 4 represents the profile of bilayer thickness change due to interactions with peptides. For peptide monomers adsorbed on the membrane surface, their effect on the membrane is expanding the area of the headgroup region. As a result, the hydrocarbon chain region also expands laterally and its thickness decreases, owing to the volume conservation. A simple way to relate peptide adsorption to thickness change is as follows. Imagine the adsorption of a peptide monomer of cross section Γ in the headgroup region, forcing a gap in the monolayer (see Fig. 7 of Ludtke et al., 1995). The volume of the gap in the chain region is Γa. To fill this gap the bilayer must become thinner locally. The decrease in the bilayer volume due to the thinning is $\int D(x,y)\, dx\, dy$. Therefore, if N_s is the total number of peptide monomers adsorbed on the membrane surface, we have

$$N_s \Gamma a = \int D(x, y)\, dx\, dy. \tag{5}$$

We will call the quantity $A = (1/a)\int D(x, y)\, dx\, dy$ the area expansion. We let the thickness change at the monomer-lipid boundary be D_s. D_s is then determined by Eq. 5. On the other hand, if the peptide is inserted, we assume that the hydrocarbon thickness matches the hydrophobic region of the inserted peptide. So the thickness change at the boundary of an inserted peptide is a fixed value D_I. The derivation of D, dD/dr, at the peptide-lipid boundary for both cases is assumed to be zero for simplicity (Huang, 1995). In principle these conditions completely define the mathematical problem of thickness deformation. The total thickness deformation energy is given by $F = \int f\, dx\, dy$.

The Gibbs free energy of membrane peptide interactions consists of three parts,

$$G = F + E_b - TS. \tag{6}$$

E_b is the binding energy, T the temperature, and S the mixing entropy. Let the total number of peptide monomers be N_p and the fraction of the peptide inserted be ϕ, so $N_s = (1 - \phi)N_p$ monomers are adsorbed on the surface and ϕN_p monomers form channels. Let n be the number of monomers comprising each channel, so that there are $N_c = \phi N_p/n$ channels. Let $-\epsilon_s$ be the binding energy of an adsorbed monomer and $-\epsilon_c$ the binding energy of one channel. Then we have $E_b = -\epsilon_s N_s - \epsilon_c N_c = N_p[(\epsilon_s - \epsilon_c/n)\phi - \epsilon_s]$. The mixing entropy is estimated by considering the monomers and the channels as distinct chemical species (Blankschtein et al., 1986),

$$S = -k_B\left[N_l \ln\left(\frac{N_l}{N_l + N_p}\right) + N_s \ln\left(\frac{N_s}{N_l + N_p}\right) + N_c \ln\left(\frac{N_c}{N_l + N_p}\right)\right], \tag{7}$$

where N_l is the number of lipid molecules and k_B is the Boltzmann constant.

The idea is to calculate the Gibbs free energy G (Eq. 6) as a function of P/L and ϕ. We expect the free energy describing an insertion phase transition to have the follow-

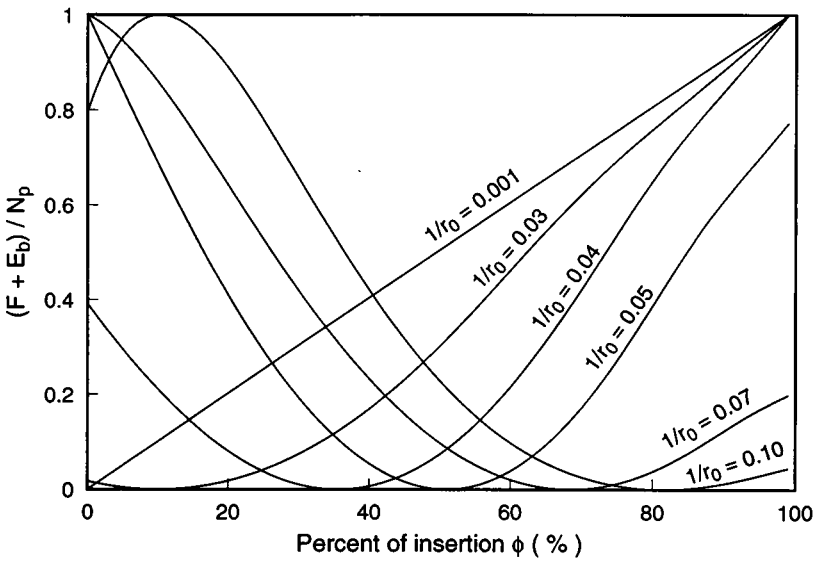

FIGURE 7 ϕ dependence of $(F + E_b)/N_p$ for various values of $1/r_o$. The scale of the energy is not normalized. The function is plotted between 0 and 1.

ing property. For small values of P/L, the minimum of G occurs at $\phi = 0$, but for P/L above a threshold value the minimum occurs at $\phi > 0$, and eventually at sufficiently high P/L the minimum occurs at $\phi = 1$. However, a rigorous proof of a phase transition is one of the most difficult tasks in statistical mechanics (e.g., Griffiths, 1972). A qualitative understanding can often be gained by considering the mathematical problem in lower dimensionalities (e.g., Huang, 1963). A one-dimensional calculation of F is carried out in Appendix II. The main results are the equation for D_s (Eq. AII 7), the equation for the average bilayer thickness change Δt (Eq. AII 8), and the thickness deformation energy F as a function of P/L and ϕ (Eq. AII 10).

The model contains the following parameters: splay (bending) constant K_c, the length scale of thickness deformation λ (or, equivalently, $1/\sqrt{2q}$), half-bilayer thickness a, the number of monomers comprising a channel n, the mismatch between the hydrophobic regions of bilayer and inserted peptide D_I, the cross section of an adsorbed monomer Γ, and the cross section of a lipid molecule w. We shall use the two-dimensional value of $\lambda = 13$ Å or $q = 5.4 \times 10^{-2}$ Å^{-1} based on the experimental values of K_c, B, and a (Chiruvolu et al., 1994; Hladky and Gruen, 1982; Huang, 1995). $a = 15$ Å for the half-bilayer thickness (Wu et al., 1995). $n = 10$ (as an approximation of 11; He et al., 1995, 1996). In the limit of high peptide concentrations, $z \to 0$, $\psi(2z) \to z$, and $\phi \to 1$, we have from Eq. AII 8, $\Delta t \to D_I$. Thus, from Fig. 5, we estimate $D_I = 2$ Å. In the limit of low concentrations, $z \to \infty$, $\psi(2z) \to 1$, and $\phi \to 0$, we obtain from Eqs. AII 7 and AII 8

$$\Delta t = \frac{a\Gamma}{w}\left(\frac{P}{L}\right), \tag{8}$$

We make use of the low concentration data in Fig. 5 where the thickness t decreases linearly with P/L with a slope equal to -105 Å. By fitting the relation in Eq. 8 to this slope, we get the ratio $\Gamma/w = 7$. The only remaining free parameters are K_c and w for the one-dimensional model.

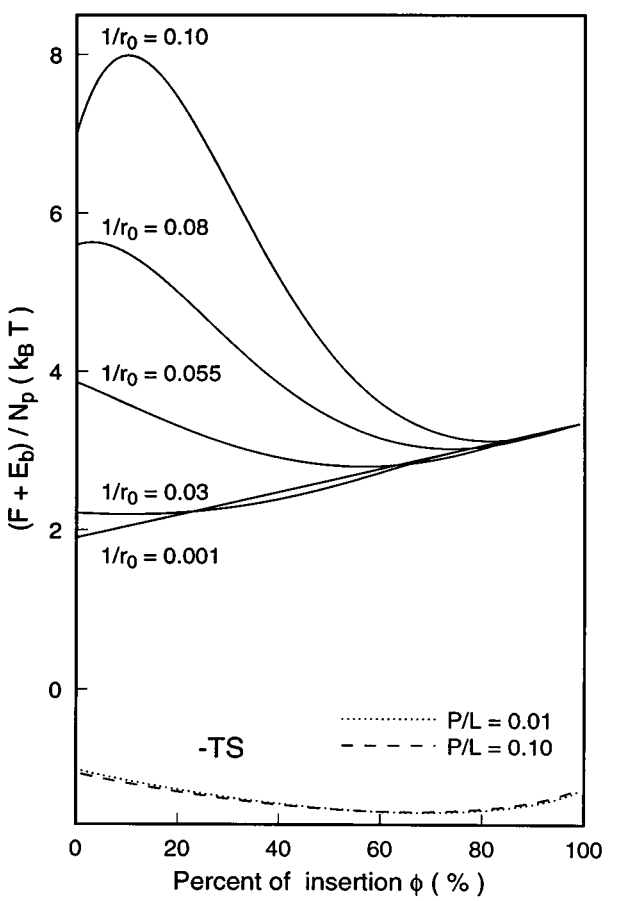

FIGURE 8 Normalized Gibbs free energy versus ϕ for various values of $1/r_o$. The entropic term is shown for P/L = 1/100 and 1/5; its ϕ dependence is insignificant compared with the energy terms.

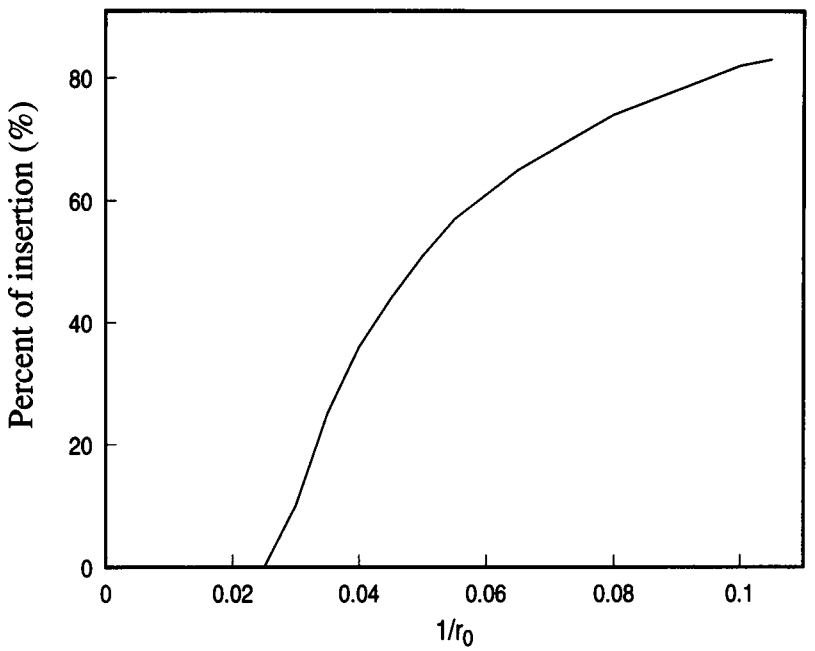

FIGURE 9 Percentage of insertion versus $1/r_o$ calculated from the one-dimensional model.

Let $r = (wN_l/N_p)/(1 - \phi + \phi/n) = r_o/(1 - \phi + \phi/n)$. r_o represents the average distance between two neighboring peptide molecules, if they were all monomers on the membrane surface. $1/r_o$ is proportional to the peptide-to-lipid ratio P/L. To see if the free energy has the expected property, we plot $(F + E_b)/N_p$ as a function of ϕ for various values of $1/r_o$ in Fig. 7. Note that E_b/N_p (as a function of ϕ) is a straight line with a constant slope equal to $\epsilon_s - \epsilon_c/n$. Provided the slope is within a certain positive range, the minimum of $(F + E_b)/N_p$ is $\phi = 0$ for small values of $1/r_o$ (low concentrations); above a threshold value of $1/r_o$, the minimum shifts to $\phi > 0$ and increases toward 1 as $1/r_o$ increases (concentration increases). To compare the relative contributions of the energetics term versus the entropic term in Eq. 6, we need to know the order of magnitude of the deformation energy. In the two-dimensional model, where all parameters are known by independent measurements, the thickness deformation energy due to the adsorption of one alamethicin monomer was calculated to be $1.9k_BT$ (Huang, 1995).

Thus we let the value of F/N_p in the limit of $1/r_o \to 0$ and $\phi \to 0$ be equal to $1.9k_BT$—this fixes the value of K_c for the one-dimensional model. The Gibbs free energy G/N_p is plotted for various values of $1/r_o$ in Fig. 8. In this figure $\epsilon_s - \epsilon_c/n$ was given a value of $3.3k_BT$, so that the threshold value of $1/r_o$ for the free energy minimum to occur at $\phi > 0$ is $1/r_o = 1/40$. This is the critical concentration for insertion, $1/r_o^*$. Changing the value of $\epsilon_s - \epsilon_c/n$ will change

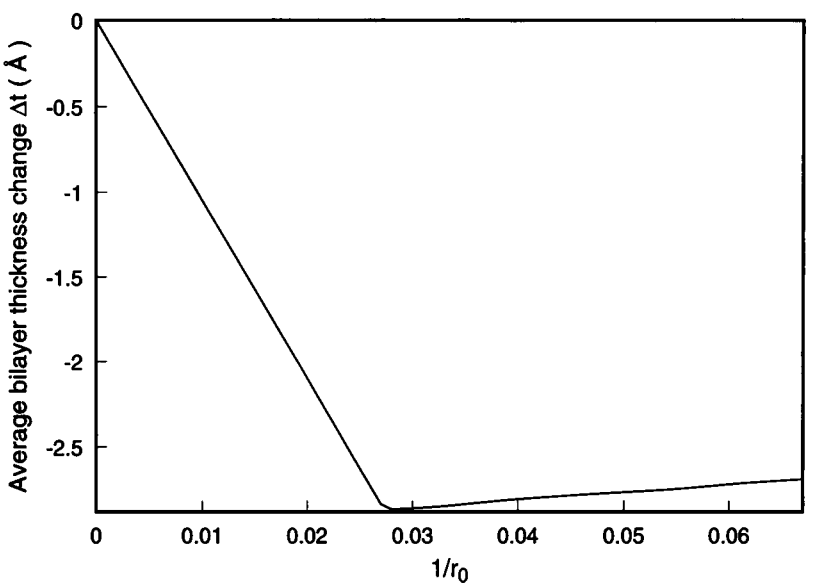

FIGURE 10 Bilayer thickness change versus $1/r_o$ calculated from the one-dimensional model.

the value of $1/r_o^*$. The entropic contributions were not included in the plotted G/N_p because they are insignificant compared with the energetics terms (see Fig. 8). The minima of G/N_p give the equilibrium value of percentage insertion as a function of $1/r_o$ (Fig. 9). The corresponding value of the average bilayer thickness change versus $1/r_o$ is given in Fig 10.

For such a crude model we certainly do not expect a quantitative agreement with the experimental data. The most important result of the model is that it exhibits an insertion phase transition. The mechanism of this transition is unlike the more familiar statistical models of order-disorder transitions, e.g., the Ising model (Huang, 1963). The latter is a transition between the (coupling) energy-dominated, low-temperature state and the entropy-dominated, high-temperature state. In contrast, the insertion transition as shown by the model is entirely driven by the energetics terms; entropy is irrelevant. The model's percentage of insertion shows the general trend of the data (Fig. 6), particularly a discontinuity from $\phi = 0$ to $\phi > 0$ at the transition point. However, whereas the data are already 100% inserted at P/L $\approx$ 1/15, the model shows only ~70% insertion at this point. The model's bilayer thickness also shows the correct general trend of the data (Fig. 5), but the details deviate from the experiment. The model predicts a minimum at the transition point, certainly not seen in the data. The rate of thickness increase in high concentrations is too small, because the percentage of insertion in the model falls behind the data. It appears that above the transition point there is not strong enough cooperativity for insertion in the model. This could be the artifact of reduced dimensionality, or the lack of a channel-channel interaction term in the free energy G. Nonetheless, the general agreement between the model and the data seems to indicate that the membrane deformation energy is the major driving force for the insertion transition.

APPENDIX I: EFFECT OF FLUCTUATION ON THE PEAK-TO-PEAK DISTANCE

Suppose that the true scattering amplitude A_h of the Bragg order h is modified by a Debye-Waller-type factor $\exp[-(\epsilon/2)(2\pi h/D)^2]$, where ϵ is a constant indicating the strength of damping. (This functional form for the fluctuation correction is a good approximation if the coherence domain for diffraction is large (He, 1996).) Then the scattering density profile ρ is

$$\rho = \sum_{h=1}^{\infty} A_h \exp\left[-\frac{\epsilon}{2}\left(\frac{2\pi h}{D}\right)^2\right] \cos\left(\frac{2\pi h}{D} z\right). \tag{AI 1}$$

At the maximum of the profile we have

$$\left(\frac{\partial \rho}{\partial z}\right)_{z=z_p} = \frac{\partial \rho}{\partial z_p} = -\sum_{h=1}^{\infty} A_h \left(\frac{2\pi h}{D}\right) \exp \left[-\frac{\epsilon}{2}\left(\frac{2\pi h}{D}\right)^2\right] \sin\left(\frac{2\pi h}{D} z_p\right) = 0, \tag{AI 2}$$

where we let the position of the maximum be z_p. Making use of the relation $\partial\rho/\partial\epsilon = \frac{1}{2}\partial^2\rho/\partial z^2$, it is easy to show that the fluctuation correction for the peak-to-peak distance t is given by

$$\delta t = 2\delta z_p = -\left(\frac{\partial^3 \rho}{\partial z_p^3} \Big/ \frac{\partial^2 \rho}{\partial z_p^2}\right)\delta\epsilon. \tag{AI 3}$$

If the peak is symmetrical ($\partial^3\rho/\partial z_p^3 = 0$), fluctuations do not affect the peak-to-peak distance.

APPENDIX II: ONE-DIMENSIONAL MODEL

Imagine a one-dimensional membrane decorated by a series of peptide monomers (adsorbed on the surface) and channels (inserted). In this model the peptide adsorptions on both sides of the membrane have exactly the same effect. The interaction between two adsorbed monomers is independent of whether they are on the same side or on opposite sides. So we may imagine that all surface monomers are adsorbed on one side of the bilayer. The bilayer thickness profile between two peptide objects (monomers or channels) is completely determined by the boundary conditions imposed by these two objects and is independent of all other peptides. If one boundary object is a monomer and the other a channel, and the distance between them is r, the thickness profile between them is given by ($x = 0$ is the midpoint)

$$D(x) = C_1 \sinh(qx)\sin(qx) + C_2 \sinh(qx)\cos(qx) + C_3 \cosh(qx)\sin(qx) + C_4 \cosh(qx)\cos(qx), \tag{AII 1}$$

with the constants

$$C_1 = \frac{(D_s + D_l)}{2} \frac{\cosh z \sin z - \sinh z \cos z}{\sinh z \cosh z + \sin z \cos z}$$

$$C_2 = \frac{(D_s - D_l)}{2} \frac{\sinh z \sin z + \cosh z \cos z}{\sinh z \cos z - \sin z \cos z}$$

$$C_3 = \frac{(D_s + D_l)}{2} \frac{\sinh z \sin z - \cosh z \cos z}{\sinh z \cosh z - \sin z \cos z} \tag{AII 2}$$

$$C_4 = \frac{(D_s - D_l)}{2} \frac{\cosh z \sin z + \sinh z \cos z}{\sinh z \cosh z + \sin z \cos z},$$

where $q = 1/\sqrt{2\lambda}$ and $z = qr/2$. If both objects are monomers, change D_l to D_s, and vice versa if both are channels. As explained in the text, D_l is a fixed value. D_s is determined as follows.

The area expansion between a channel and an adsorbed monomer is

$$A_{SI} = \frac{1}{a}\int_{-r/2}^{r/2} D\,dx = \frac{(D_s + D_l)}{aq} \frac{\cosh(2z) - \cos(2z)}{\sinh(2z) + \sin(2z)}. \tag{AII 3}$$

The area expansion between two channels A_{II} is obtained by replacing D_s by D_l. Similarly, A_{ss} between two monomers is obtained by replacing D_l by D_s.

As a mean field theory, we will assume that the peptide objects are equally spaced on the membrane, but the monomers and channels are otherwise randomly distributed. Let wN_l (N_l is the total number of lipid molecules) be the length of the one-dimensional membrane. Then the average interpeptide distance is $r = wN_l/(N_s + N_c) = w/[(P/L)(1 - \phi + \phi/n)]$, where P/L = N_p/N_l is the peptide-lipid ratio. For a given P/L and ϕ, we will calculate the area expansion due to the adsorbed monomers (denoted as A_1) and equate it to $N_s\Gamma$—this relation will determine D_s. The

total area expansion A_T is partly due to the channels (denoted as A_2): $A_1 = A_T - A_2$. A_T is given by

$$A_T = \frac{1}{N_s + N_c}(N_s^2 A_{ss} + 2N_s N_I A_{sI} + N_I^2 A_{II}) = \frac{2N_p}{aq}\left[\frac{\phi}{n} D_I + (1 - \phi)D_s\right]\psi(2z), \quad \text{(AII 4)}$$

where

$$\psi(z) = \frac{\cosh(z) - \cos(z)}{\sinh(z) + \sin(z)}. \quad \text{(AII 5)}$$

If all of the surface monomers were removed, the area expansion by the channels alone is given by

$$A_2 = \frac{\phi N_p}{n}\frac{2D_I}{aq}\psi(2z_I), \quad \text{(AII 6)}$$

where $z_I = qr_I/2$ and $r_I = wN_I/N_c = w/[(P/L)(\phi/n)]$ is the mean distance between neighboring channels. Thus $N_s\Gamma = A_1$ becomes

$$D_s = \frac{1}{\psi(2z)} D_0 - \frac{\phi}{(1 - \phi)n}\left[1 - \frac{\psi(2z_I)}{\psi(2z)}\right]D_I, \quad \text{(AII 7)}$$

where $D_0 = aq\Gamma/2$.

We define the average bilayer thickness change as

$$\Delta t = \frac{\int D(x)\,dx}{\int dx} = \frac{[(\phi/n) D_I + (1 - \phi)D_s]}{(\phi/n) + (1 - \phi)}\frac{\psi(2z)}{z}. \quad \text{(AII 8)}$$

To calculate the deformation energy between a monomer and a channel, we substitute Eqs. AII 1 and AII 2 into Eq. 3 and integrate from $-r/2$ to $r/2$:

$$F_{sI} = \int_{-r/2}^{r/2} f\,dx = \frac{K_c q^3}{4}\left[(D_s + D_I)^2\frac{\cosh(2z) - \cos(2z)}{\sinh(2z) + \sin(2z)} + (D_s - D_I)^2\frac{\cosh(2z) + \cos(2z)}{\sinh(2z) - \sin(2z)}\right]. \quad \text{(AII 9)}$$

For the energy between two monomers F_{ss}, D_I is replaced by D_s, and vice versa for the energy between two channels F_{II}. The total thickness deformation energy is

$$F = \frac{1}{N_s + N_c}(N_s^2 F_{ss} + 2N_s N_I F_{sI} + N_I^2 F_{II}) = \frac{N_p}{1 - \phi + (\phi/n)}\left[(1 - \phi)^2 F_{ss} + \frac{2\phi(1 - \phi)}{n} F_{sI} + \frac{\phi^2}{n^2} F_{II}\right]. \quad \text{(AII 10)}$$

This work was supported in part by National Institutes of Health grant AI34367 and Biophysics Training grant GM08280, by Department of Energy grant DE-FG03-93ER61565, and by the Robert A. Welch Foundation.

REFERENCES

Asher, S. A., and P. S. Pershan. 1979. Alignment and defect structures in oriented phosphatidylcholine multilayers. *Biophys. J.* 27:137–152.

Blankschtein, D., G. M. Thurston, and G. B. Benedek. 1986. Phenomenological theory of equilibrium thermodynamic properties and phase separation of micellar solutions. *J. Chem. Phys.* 85:7268–7288.

Caillé, A. 1972. Remarques sur la diffusion des rayons X dans les smectiques. *C. R. Acad. Sci. (Paris) Série B.* 274:891–893.

Chiruvolu, S., H. E. Warriner, E. Naranjo, S. Idziak, J. O. Radler, R. J. Plano, J. A. Zasadzinski, and C. R Safinya. 1994. A phase of liposomes with entangled tubular vesicles. *Science.* 266:1222–1225.

Griffiths, R. B. 1972. Rigorous results and theorems. *In* Phase Transitions and Critical Phenomena, Vol. 1. C. Domb and M. S. Green, editors. Academic Press, New York. 8–109.

He, K. 1996. Studies of amphiphilic helical peptides interacting with lipid bilayer membranes by x-ray and neutron scattering. Ph.D. thesis. Rice University, Houston, TX.

He, K., S. J. Ludtke, D. L. Worcester, and H. W. Huang. 1995. Antimicrobial peptide pores in membranes detected by neutron in-plane scattering. *Biochemistry.* 34:16764–16769.

He, K., S. J. Ludtke, D. L. Worcester, and H. W. Huang. 1996. Neutron scattering in the plane of membranes: structure of alamethicin pores. *Biophys. J.* 70:2659–2666.

Helfrich, W. 1973. Elastic properties of lipid bilayers: theory and possible experiment. *Z. Naturforsch.* 28C:693–703.

Hladky, S. B., and D. W. R. Gruen. 1982. Thickness fluctuations in black lipid membranes. *Biophys. J.* 38:251–258.

Huang, H. W. 1995. Elasticity of lipid bilayer interaction with amphiphilic helical peptides. *J. Phys. II France.* 5:1427–1431.

Huang, H. W., K. He, W. T. Heller, and S. J. Ludtke. 1995. Interaction of Lipid Bilayer Membranes with Amphiphilic Helical Peptides in Short and Long Chains at Interfaces. J. Daillant, P. Guenoun, C. Marques, P. Muller, and J. Vân, editors. Editions Frontieres, Gif-sur-Yvette. 339–344.

Huang, H. W., and G. A. Olah. 1987. Uniformly oriented gramicidin channels embedded in thick monodomain lecithin multilayers. *Biophys. J.* 51:989–992.

Huang, H. W., and Y. Wu. 1991. Lipid-alamethicin interactions influence alamethicin orientation. *Biophys. J.* 60:1079–1087.

Huang, K. 1963. Statistical Mechanics. John Wiley and Sons, New York. 352–361.

Jen, W.-C., G. A. Jones, D. Brewer, V. O. Parkinson, and A. Taylor. 1987. The antibacterial activity of alamethicin and zervamicins. *J. Appl. Bacteriol.* 63:293–298.

Latorre, R., and S. Alvarez. 1981. Voltage-dependent channels in planar lipid bilayer membranes. *Physiol. Rev.* 61:77–150.

Lei, N., C. R. Safinya, and R. F. Bruinsma. 1995. Discrete harmonic model for stacked membranes: theory and experiment. *J. Phys. II (France).* 5:1155–1163.

Ludtke, S., K. He, and H. W. Huang. 1995. Membrane thinning caused by magainin 2. *Biochemistry.* 34:16764–16769.

Ludtke, S. J., K. He, Y. Wu, and H. W. Huang. 1994. Cooperative membrane insertion of magainin correlated with its cytolytic activity. *Biochim. Biophys. Acta.* 1190:181–184.

Mak, D. D., and W. W. Webb. 1995. Two classes of alamethicin transmembrane channels: molecular models form single-channel properties. *Biophys. J.* 69:2323–2336.

Meyer, P., and F. Reusser. 1967. A polypeptide antibacterial agent isolated from *Trichoderma viride. Experientia.* 23:85–86.

Nagle, J. F., R. Zhang, S. Tristram-Nagle, W. Sun, H. I. Petrache, and R. M. Suter. 1996. X-ray structure determination of fully hydrated L_a phase dipalmitoylphosphatidylcholine bilayers. *Biophys. J.* 70:1419–1431.

Nallet, F., R. Laversanne, and D. Roux. 1993. Modelling x-ray or neutron scattering spectra of lyotropic lamellar phases: interplay between form and structure factors. *J. Phys. II France.* 3:487–502.

Olah, G. A., and H. W. Huang. 1988. Circular dichroism of oriented alpha helices. I. Proof of the exciton theory. *J. Chem. Phys.* 89:2531–2538.

Pandey, R. C., J. C. Cook, and K. L. Rinehart. 1977. High resolution and field desorption mass spectrometry studies and revised structure of alamethicin I and II. *J. Am. Chem. Soc.* 99:8469–8483.

Vogel, H. 1987. Comparison of the conformation and orientation of alamethicin and melittin in lipid membranes. *Biochemistry.* 26: 4562–4572.

Wu, Y., K. He, S. J. Ludtke, and H. W. Huang. 1995. X-ray diffraction study of lipid bilayer membrane interacting with amphiphilic helical peptides: diphytanoyl phosphatidylcholine with alamethicin at low concentrations. *Biophys. J.* 68:2361–2369.

Wu, Y., H. W. Huang, and G. A. Olah. 1990. Method of oriented circular dichroism. *Biophys. J.* 57:797–806.

Zhang, R., R. M. Suter, and J. F. Nagle. 1994. Theory of the structure factor of lipid bilayers. *Physiol. Rev.* E50:5047–5060.